PASSIVE/ACTIVE MICROWAVE SOIL MOISTURE CHANGE DISAGGREGATION USING SMAPVEX12 DATA

Bin Fang*
Venkat Lakshmi
Earth and Ocean Sciences, University of South Carolina
Columbia SC 29223
* Corresponding author bfang@geol.sc.edu

Thomas J Jackson
Hydrology and Remote Sensing Laboratory, Beltsville Agricultural Research Center, United States Department of Agriculture, Beltsville MD 20705

Rajat Bindlish
NASA Goddard Space Flight Center, Greenbelt, MD 20771

Andreas Colliander
Jet Propulsion Laboratory, California Institute of Technology, Pasadena, CA 91109

ABSTRACT

The SMAPVEX12 (Soil Moisture Active Passive (SMAP) Validation Experiment 2012) experiment was conducted during June-July 2012 in Manitoba, Canada with the goal of collecting remote sensing data and ground measurements for the development and testing of soil moisture retrieval algorithms under varying vegetation and soil conditions for the SMAP satellite. The aircraft based soil moisture data provided by the passive/active microwave sensor PALS (Passive and Active L-band System) has a nominal spatial resolution of 1600 m. However, this resolution is not compatible with agricultural, meteorological and hydrological studies that require high spatial resolutions and this issue can be solved by soil moisture disaggregation. The soil moisture disaggregation algorithm integrates radiometer soil moisture retrievals and high-resolution radar observations and it can provide soil moisture estimates at a finer scale than the radiometer data alone. In this study, a change detection algorithm was used for disaggregation of coarse resolution passive microwave soil moisture retrievals with radar backscatter coefficients obtained from the higher spatial resolution UAVSAR (Unmanned Air Vehicle Synthetic Aperture Radar) at crop field scale. The accuracy of the disaggregated change in soil moisture was evaluated using ground based soil moisture measurements collected during SMAPVEX12 campaign. The results showed that soil moisture spatial variabilities were better characterized by the disaggregated change in soil moisture estimates at 5 m / 800 m resolution as well as good agreement with *in situ* measurements. It also showed that VWC (Vegetation Water Content) did not have a big impact on disaggregation algorithm performance, with R^2 of the disaggregated results ranging 0.628-0.794. The 5 m and 800m

resolution disaggregated soil moisture did no show significant difference in statistical performance variables.

Keywords: SMAP, Microwave soil moisture, radar backscatter, disaggregation change detection algorithm.

1 INTRODUCTION

Soil moisture is important in agriculture, land-atmosphere interactions, hydrology and ecology (Lakshmi, 2004, 2013). Microwave remote sensing technology has been providing soil moisture retrievals with improving capabilities for many land surface hydrological applications (Lakshmi et al., 2004) since the late 1970s (Schmugge et al., 1974; Jackson and Schmugge. 1989; Jackson 1993; Njoku et al., 1996; Schmugge et al., 2002). Soil moisture algorithms have been developed (Schmugge and Jackson, 1994; Wigneron et al., 1995; Jackson et al., 2002; Kerr et al., 2007; Njoku et al., 1999, 2003), applied and assessed by passive microwave sensors onboard satellites, including the SSM/I (Special Sensor Microwave - Imager), TRMM (Tropical Rainfall Measuring Mission) and WindSAT. In recent two decades, soil moisture retrievals were acquired from airborne sensors such as Electronically Scanned Thinned Array Radiometer (ESTAR) (Jackson et al., 1999) as well as passive microwave satellite missions AMSR-E (Advanced Microwave Scanning Radiometer for the Earth Observing System), AMSR2 (Advanced Microwave Scanning Radiometer 2), SMOS (Soil Moisture and Ocean Salinity), Aquarius on board the satellite SAC-D (Satélite de Aplicaciones Científicas-D) and the recently launched satellite SMAP (Soil Moisture Active Passive). With the development of the remote sensing soil moisture, numerous field campaigns have been conducted to support the validation of these soil moisture products (Jackson et al., 2010, 2012; Peischl et al., 2009; Mladenova et al., 2010, 2011), develop improved soil moisture retrieval algorithms and study the scaling properties (Rodríguez et al., 1995; Mohanty et al., 2000; Cosh et al., 2004; Heathman et al., 2012; Minet et al., 2012) as well as the impacts from land surface objects (Njoku et al., 2006;) on satellite soil moisture observations.

The spatial resolution of the passive soil moisture products has been restricted by the diameter of the antenna and the observing altitude, and as a result, their spatial resolution is typically at tens of kilometers for space-borne products. These products cannot meet all of the requirements for researches and applications that require higher spatial resolutions. With a goal of overcoming this problem, the SMAP mission was developed by NASA (National Aeronautics and Space Administration) and launched in January 2015. The SMAP satellite provided radiometer soil moisture products with multiple spatial resolutions at 9 / 36 km (Entekhabi et al., 2010). However, due to an anomaly, the radar ended operation in July 2015 and the best resolution available now is at 36 km. There are enhanced products with a 9 km grid cell size based solely on the radiometer data. In order to support evaluation and test of candidate SMAP soil moisture retrieval algorithms, a pre-launch field campaign was carried out from June 6 - July 19, 2012 in southern Manitoba, Canada that provided remotely sensed data from two aircraft systems PALS (Passive Active L-band System) and UAVSAR (Uninhabited Aerial Vehicle Synthetic Aperture Radar), as well as ground soil moisture measurements from field sampling and permanent soil moisture monitoring network stations (McNairn et al., 2015; Xu et al., 2014).

Soil moisture disaggregation algorithms have been proposed based on several techniques that utilize physical principles deriving disaggregating information from microwave radiometer/radar instruments (Lakshmi 2013). These include using triangular relationship between land surface temperature, soil moisture and vegetation (Gillies et al., 1995; Carlson et al., 1995, 2007; Luo et al., 2007; Mallick et al., 2009; Minacapilli et al., 2009; Lakshmi et al., 2011). Various approaches utilized satellite retrieved high spatial resolution land surface variable estimates from visible/infrared band combinations, such as

Land Surface Temperature (LST) and Vegetation Indices (VI) to disaggregate soil moisture. For instance, the MODIS NDVI (Normalized Difference Vegetation Index), LST and brightness temperature (T_B) could be statistically combined for building disaggregating models (Piles et al., 2009, 2011; Kim et al., 2012; Choi et al., 2012; Fang et al., 2013; Fang et al., 2014a; Sánchez-Ruiz et al., 2014; Fang et al., 2018a, Fang et al., 2018b). On another hand, the other soil moisture related variables derived from satellite estimates, such as Soil Evaporation Efficiency (SEE) could also be considered. The relationship between soil moisture and SEE was investigated and high resolution remotely sensed SEE estimates were utilized for disaggregating passive microwave soil moisture (Merlin et al., 2008, 2009, 2010, 2012, 2013), as well as a follow-up variant approach proposed by Fang et al., 2014b. An algorithm which is based on the Universal Triangle approach used optical/infrared remote sensing derived variables to build the linkage model for disaggregating SSM/I soil moisture (Chauhan et al., 2003). This approach was also applied for disaggregating AMSR-E soil moisture using MODIS products (Yu et al., 2008) and then applied to mapping landslide susceptibility (Ray et al., 2010). Additionally, the microwave soil moisture could also be disaggregated using statistical or data assimilation approaches (Parada et al., 2004; Pan et al., 2009; Sahoo et al., 2013; Zhao et al., 2013; Peng et al., 2017).

Radars, especially synthetic aperture satellite systems, can provide much higher spatial resolution data than radiometers, because they use the distance traveled by the antenna between the send and receive pulses to synthesize a large antenna. However, it can be more difficult to retrieve soil moisture directly from radar backscatter coefficients, because the interaction with the target is more complicated and is related to vegetation canopy structure and soil surface roughness (Bindlish et al., 2002). There have been prior

investigations on the retrieval of soil moisture from active/passive microwave observations (Schmugge et al., 1974; Choudhury et al., 1979; Njoku and Entekhabi, 1996; Lakshmi et al., 1997), as well as soil moisture disaggregating studies by integrating high resolution radar data with passive microwave soil moisture products published by Bolten et al., 2003; Narayan et al., 2004, 2008; Das et al., 2011)

Here, we focus on a radar-based change detection approach for disaggregating soil moisture retrievals at field scale. Previous studies have shown the potential of using this method to determine the change in soil moisture or relative soil moisture (Engman and Chauhan, 1995; Njoku, et al, 2002; Ujjwal et al., 2006). The change detection method assumes that the change in radiometer T_B or radar backscatter recorded by the sensor only depends on the change in soil moisture of the target for successive observations over short periods of time (< 5 days) at field scale. These studies have shown that there is a linear relationship between the change in T_B / radar backscatter and the change in soil moisture (Njoku et al., 1999; Narayan et al., 2006).

In this study, a change detection algorithm was implemented to disaggregate the PALS passive based soil moisture retrievals by combining them with high-resolution UAVSAR radar backscatter observations at 5/800 m aggregation. This methodology assumes that the influence of the spatial and temporal heterogeneity of soil properties can be ignored, as well as the variability of radar backscatter within the radiometer pixel only depends on soil moisture and vegetation water content. The novel contribution of this study is that the coarse resolution passive microwave PALS change in soil moisture at 1600 m is disaggregated by applying the change detection algorithm to high-resolution UAVSAR radar observations, without using other ancillary data. Respectively, the two resolutions

are 5 m, which is the finest resolution of UAVSAR for studying the algorithm performance by crop types, as well as 800 m which corresponds to the crop field size. This approach would provide a possible solution for estimating higher spatial resolution soil moisture in change by combining L-band radiometer soil moisture retrievals and L-band radar observations.

2 STUDY AREA AND DATA

The SMAPVEX12 campaign was held in the southern portion of Manitoba province, Canada, centered on the town of Elm Creek (98º0'23" W, 49º40'48" N), covering a rectangular region of 12.8 km wide by 70 km long (Figure 1). The campaign area is mainly located in the Canadian Red River Watershed and partly in the Assiniboine Watershed and Lake Winnipegosis / Lake Manitoba Watershed. The campaign area has the desired mix of land covers and the soil texture is dominated by sand in the west and loam and silt in the east. The major landscape types in the study area include crops such as soybeans, wheat, corn, canola and pasture, as well as some wetland and forests present in the watershed. Each crop field is 800 × 800 m (a quarter section). In this study, remote sensing data and *in situ* measurements were collected covering 55 agricultural fields (McNairn et al., 2015). The data sets used for retrieving and disaggregating microwave soil moisture are listed in Table 1.

2.1 PALS RADIOMETER/RADAR DATA

The PALS (Passive Active L-band System) was used to simulate SMAP observations during the SMAPVEX12 campaign. This instrument was mounted on a Twin Otter aircraft with a 40-degree viewing angle. During the SMAPVEX12 experiment, the

PALS provided two sets of observations, L-band (1.413 GHz) radiometer T_B at horizontal (H) and vertical (V) polarizations (Colliander, 2013a) and L-band (1.26 GHz) radar backscatter coefficients at VV, HH, VH and HV polarizations (Colliander, 2013b; Kim et al., 2015). Data were acquired at two elevations (1372 m for low elevation and 2896 m for high elevation) with along-track spatial resolutions of approximately 655 m and 1592 m, respectively (McNairn et al., 2015). Only limited areas were covered at low altitude but the entire experimental domain was mapped at high altitude for better visualizing soil moisture spatial pattern. In this article, the PALS high elevation flight radiometer soil moisture retrievals at 1600 m, which were computed by the approach of Colliander et al. (2016) were selected for implementing the disaggregation algorithm.

The daily-accumulated precipitation measurements from the local weather station network were compared with the average PALS radiometer and radar observations at H and V polarizations in the study area in Figure 2. During the experiment, Heavy precipitation events occurred in mid-June, June 27, and July 19, as well as follow-up fast soil moisture dry-down occurred before July 1. It is clear that the PALS T_B was inversely related to the *in situ* soil moisture, while the radar backscatter response was more complex. The radar backscatter generally had a positive correlation to the *in situ* soil moisture, but the temporal inconsistency between the two data sets could be noted. This was probably because the cropland might have lag effect to the precipitation and the radar signal did not timely respond to the soil moisture change (Niu et al., 2015). In addition, crop irrigation from June 29 – July 19 contributed extra soil moisture to the study area and consequently the inconsistent responses between the rain gauge precipitation, PALS observations and *in situ* soil moisture can be noticed in Figure 2. Several factors: precipitation, temperature,

irrigation and crop evapotranspiration might contribute to the soil moisture change. Therefore, the wetting trend occurred in July 5 of the day with no rain might be due to the irrigation.

2.2 UAVSAR DATA

The UAVSAR is a fully-polarimetric and interferometric L-band radar. It operates at approximately the same frequency as PALS (1.26 GHz), and has a spatial resolution of 1.66 m in range scale and 3 m in the multi-look angle mode. During the SMAPVEX12, The UAVSAR sensor was on board NASA Gulfstream III (G-III) Research Testbed Aircraft and the nominal flight altitude was 13 km (McNairn et al., 2015). The incidence angle of UAVSAR was between 25-65 degrees and had a swath width of 3.8 km (http://uavsar.jpl.nasa.gov/). Since the incidence angle contributes to the response and SMAP has a fixed incidence angle of 40 degrees, we utilized the data of normalized incidence angle at 40 degrees which is proposed by Xu at al., 2014. These incidence-angle-normalized UAVSAR radar backscatter observations of HH polarization were resampled to 5 m and were downloaded from http://uavsar.jpl.nasa.gov/cgi-bin/data.pl. In order to study the soil moisture spatial and temporal variability at the sampling fields scale, the 5 m data was also aggregated to 800 m to implement the change detection algorithm.

2.3 VEGETATION WATER CONTENT

The VWC data was calculated from the NDWI (Normalized Difference Water Index) products derived from 5 m spatial resolution satellite imagery (SPOT, Satellite Pour l'Observation de la Terre) and RapidEye, covering the SMAPVEX12 field sampling and flight days from June through July 2012 (Cosh, 2015). For each major crop type, the daily SPOT and RapidEye NDVI (Normalized Difference Vegetation Index) data were

compared to the daily field sampled VWC measurements. A linear interpolation was applied to fit the relationship and then calculate the VWC at 5 m resolution (McNairn et al., 2015). In this study, we used VWC data at 5 m and 800 m resolution for implementing soil moisture disaggregation and VWC at 1600 m for building the model between change in PALS soil moisture and change in UAVSAR radar backscatter coefficient.

2.4 *IN SITU* SOIL MOISTURE OBSERVATIONS

In order to obtain representative soil moisture estimates for each SMAPVEX fields, the volumetric soil moistures were collected using handheld Hydra probes at multiple locations (Wiseman et al., 2014, McNairn et al., 2015). A total of 60 crop and pasture fields and 5 forest sites were visited each day during the SMAPVEX12 campaign and the soil moisture measurements were acquired on the days that coincided with aircraft flight overpasses. For each field, soil moisture was measured at 16 sampling points along two transects of 8 points that were parallel to the crop row direction, with three replicate measurements at each of these sample points.

3 METHODOLOGY

Data flow of this study is as shown in Figure 3. Both L-band radiometer T_B and radar backscatter have nearly linear relationships to skin surface soil moisture under uniform vegetation and land surface conditions (Narayan et al., 2006). Soil moisture retrieval using radiometer observations is well established and here we used the PALS soil moisture retrievals by the method of Colliander et al. (2016) with a spatial resolution of 1600 m.

As mentioned above, the dependence of the radar backscatter on the change of soil moisture can be simplified by assuming a linear relationship. Njoku et al. (2002) modeled the relationship between the PALS radiometer / radar data acquired from SGP99 (1999 Southern Great Plains Experiment) campaign, which were at the same size of footprint. The PALS data and *in situ* soil moisture measurements were classified into 3 different classes by the vegetation water content and modeled the linear regression relationship individually. The modeled equations are

$$T_{B_P} = A + B\theta \qquad (1)$$

$$\sigma^o_{PP} = C + D\theta \qquad (2)$$

Where brightness temperature is T_{B_P}, radar backscatter σ^o_{PP} and soil moisture is θ. A, B, C and D are regression parameters that correspond to each PALS radiometer or radar pixel. They were assumed to be functions of surface vegetation and roughness. For the Equation 2, the parameters C and D can be calibrated by the soil moisture change on consecutive days. Here, the purpose is to estimate the soil moisture change at the spatial resolution of radar by combining PALS radiometer soil moisture with the radar backscatter observations. In this study, the PALS soil moisture is at 1600 m resolution while the UAVSAR backscatter is at 5 m/800 m resolution. It is our assumption that during a short period (a few days), the changes in the vegetation canopy can be ignored and the changes in the co-polarized radar backscatter result from soil moisture only.

Both the PALS and UAVSAR observations were obtained at a high revisit frequency over the study region. The linear relationship between the change in soil moisture and the change in radar backscatter can be expressed as

$$\Delta\sigma^o_{PP} = D\Delta\theta \qquad (3)$$

Where, $\Delta\sigma^0_{PP}$ is the co-polarized change in radar backscatter and $\Delta\theta$ is the change in soil moisture. The parameter D depends on the attenuation properties of the vegetation canopy and soil surface roughness characteristics. Previous research (Du et al., 2000) demonstrated that the relative sensitivity of radar backscatter to soil moisture primarily depends on the vegetation canopy opacity, which can be described as the ratio of the radar sensitivity in the presence of vegetation canopy (D) to the sensitivity if there was only bare soil (D_0), as

$$\frac{D}{D_0} = f(\tau) \qquad (4)$$

Combining the Equations 3 and 4, we have

$$\Delta\sigma^0_{PP} = f(\tau) * D_0 * \Delta\theta \qquad (5)$$

The radar sensitivity of bare soil (D_0) is determined by the soil roughness variability for a specific sensor configuration: look angle, frequency and polarization. In the study by Fung et al (1992), the curves representing the relationship between the L-band horizontally co-polarized radar backscattering coefficients and soil moisture under different root mean square soil surface roughness conditions s (cm) from s = 0.4~2.4 cm were found to be nearly parallel, with the same slope but different intercepts. This indicates that the influence of soil surface roughness on the soil moisture sensitivity of radar can be ignored. Equation 5 can be simplified as

$$\Delta\theta = \frac{\Delta\sigma^0}{S_0} \qquad (6)$$

Where, $S_0 = f(\tau) * D_0$. The soil moisture derived from the passive microwave data is available at the coarser spatial resolution (1600 m) and derived from the radar backscatter data is at a finer spatial resolution (5 m / 800 m). To disaggregate the change in soil moisture to a finer resolution, the soil moisture difference was calculated from two PALS radiometer soil moisture images (1600 m) on two days t_0 to $t_0 + \Delta t$.

$$\Delta\theta^{low} = \left(\frac{1}{N}\right) \sum \Delta\theta^{high} \quad (7)$$

Where, $\Delta\theta^{low}$ is the low spatial resolution PALS radiometer soil moisture change, which is based on "N" fine resolution radar pixels, while $\Delta\theta^{high}$ is the radar backscatter disaggregated soil moisture to the high spatial resolution. Combining Equation 6 with Equation 7 we obtain

$$\Delta\theta^{low} = \left(\frac{1}{N}\right) \sum \left[\frac{\Delta\sigma_0^{high}}{S_0}\right] \quad (8)$$

The average is over the changes of all "N" smaller UAVSAR radar footprints σ_0^{high} within the larger radiometer footprint. This is the change in soil moisture measured by the radiometer at the low spatial resolution (1600 m), in terms of the change in soil moisture measured by the radar at the high spatial resolution (5 m /800 m).

The PALS/UAVSAR data were collected over crop fields, so we made an assumption that the slope S_0 would be the same for all the radar pixels falling in one radiometer pixel when given uniform land cover condition, so soil roughness and vegetation characteristics can be linearly averaged. The SMAPVEX12 experiment provided agricultural fields with uniform vegetation characteristics. Thereby, given a very short time period, the spatial and temporal variability of vegetation canopy parameters should have limited influence on the variability of the radar signals within the radiometer pixel. And, only the variability of soil moisture and canopy vegetation water content would account for the variability of radar signals within the corresponding radiometer pixel. Furthermore, this assumption is based on a previous publication by Narayan et al., 2006 who proved that the soil surface radar sensitivity at subpixel scale did not have a big impact on the radar sensitivity to soil moisture. According to their approach, the coarse resolution PALS radiometer soil moisture estimates were

disaggregated using high resolution radar observations from AIRSAR (Airborne Synthetic Aperture Radar) and the validation results showed the overall mean square error of predicted estimates ranged between 0.02-0.03 m^3/m^3.

Equation 8 can be transformed as

$$S_0 = (\frac{1}{N}) \frac{\Sigma \Delta \sigma_0^{high}}{\Delta \theta^{low}} \quad (9)$$

Based on the assumption mentioned above, the S_0 would be the same for all the pixels at the radar backscatter resolution (5 m/800 m) within the corresponding 1600 m resolution radiometer pixel. The soil moisture change $\Delta\theta^{high}$ at high resolution can be calculated as

$$\Delta\theta^{high} = \frac{\Delta \sigma_0^{high}}{S_0} \quad (10)$$

by applying the slope S_0 derived from the correlation line between PALS $\Delta\Theta$ and summation of UAVSAR $\Delta\sigma^0$ (5 m/800 m) at 1600 m resolution.

4 RESULTS

4.1 PALS SOIL MOISTURE RETRIEVALS

The passive microwave soil moistures were retrieved using $\tau - \omega$ model based retrieval algorithm (Colliander et al., 2016). The PALS radiometer soil moisture retrievals are at a 1600 m spatial resolution for the six sampling days: June 15, June 22, July 13, July 14 and July 19 as shown in Figure 4. The soil moisture was approximately 0.2 m^3/m^3 lower in the northern part of the flight path than the southern for all of the days. The southern portion showed higher spatial and temporal variability of soil moisture. (Colliander et al., 2015). These features were probably due to the different land cover types. The northern

region is dominated by forest and grasslands where tends to show stable temporal soil moisture variability, while the southern region is covered by various types of crop fields. (Zucco et al., 2014; Niu et al., 2015). Additionally, the soil types in the south are clay and loam which have better water-holding ability than in the north and showed wetter condition. Inconsistencies between *in situ* soil moisture shown in Figure 2 and PALS soil moisture maps in Figure 4 can be noted. Firstly, June 22 was generally wetter than June 15. The reason could be June 15 was the day between two major precipitation events and a fast soil moisture dry-down occurred, while the soil moisture dry-down rate was slower and little precipitation occurred in June 22. Additionally, we may also find that a major precipitation occurred in July 19 in Figure 2, but the soil moisture was not as high as in June 15 and 22. This probably because of soil moisture in croplands might slowly respond to the precipitation. And, for the SMAPVEX12 site, soil moisture in July was basically lower than in June as a persistent dry-down trend was shown in Figure 3.

Figure 5 shows the maps of the data sets used in soil moisture disaggregation and the other related land surface variables in July 10 - July 13. A clear wetting trend of increased soil moisture, which was approximately 0.2 m^3/m^3, can be seen in the center of the flight path and a soil moisture dry-down in the southern part, where was dominated by crop fields (Figure 5-i). The PALS and UAVSAR changes in radar backscatter (Figure 5-ii, 5-iii) were positively correlated to changes in soil moisture. The VWC (Figure 5-iv) composited from multiple flight days showed a region of high VWC associated with the presence of forest cover in the northern portion of the study area. As opposed to the Northern region, the VWC ranged from 0-4 kg/m^2 and demonstrated less spatial variation in the southern part of the study area. For the LST and NDVI derived from MODIS (Figure

5-v, 5-vi), the north and south regions distinctly had different spatial patterns. The north region, where was largely covered by grassland and pasture, had higher temperature but lower NDVI (only except part of central north region covered by forest), while the south region was dominated by crop fields and had lower temperature and higher NDVI.

In situ observations at sampling sites collected during the campaign were used to validate the retrieved soil moisture from PALS at 1600 m, as well as the disaggregated soil moisture using UAVSAR radar backscatter at 5 m and 800 m. The ground sampled soil moisture was gridded to the PALS and UAVSAR pixel scales by averaging all the point soil moisture measurements falling in the corresponding pixel. The vegetation water content data aggregated to the PALS and UAVSAR pixel scales was divided into four classes in order to study the impact of VWC on the accuracy of retrieved and disaggregated PALS soil moisture.

In this study, the statistical variables include R^2, slope and its 95% confidence interval, RMSE (Root Mean Square Error), unbiased RMSE, bias, and spatial standard deviation, which is used to examine spatial variability of the estimated change in soil moisture).

From Table 2, it could be observed that the R^2 values of the PALS soil moisture retrieval validation for the two VWC intervals of 1.5-2 kg/m^2 and 2-2.5 kg/m^2 which are 0.726 and 0.772 respectively, are better than these of the other two classes of 0-1.5 kg/m^2 and >2.5 kg/m^2. The slopes for all the VWC classes range between 0.818-1.192 and they are close to the 1:1 line. Regarding to the other variables, the RMSE ranges from 0.066-0.072 m^3/m^3, unbiased RMSE ranges from 0.025-0.033 m^3/m^3, and bias ranges from 0.015-0.033 m^3/m^3, which all indicate good accuracy of the PALS soil moisture retrievals. The

95% confidence interval, RMSE and bias do not vary much between the different VWC classes. In addition, the PALS soil moisture shows a general underestimation tendency.

4.2 COMPARISON BETWEEN PALS SOIL MOISTURE RETRIEVALS AND UAVSAR RADAR BACKSCATTER

Figure 6 shows the scatter plots of the PALS change in soil moisture versus the (a) PALS change in backscatter and (b) aggregated UAVSAR change in backscatter at 1600 m. The R^2 of the PALS comparisons approximately range between 0.68-0.77, while the R^2 of the UAVSAR comparisons range between 0.6-0.76. The PALS backscatter observations were co-incident with PALS radiometer estimates soil moisture retrievals, while the UAVSAR observations were processed to match the PALS observations with the same incidence angle and resolution. In addition, we may also note that there is a slight difference in the slope S_0 between UAVSAR and PALS comparisons each day. The S_0 of the PALS comparison, ranging from 13.87-14.64, is generally greater than the corresponding UAVSAR comparison (9.04-14.07). The different incidence angles and original spatial resolutions of PALS and UAVSAR sensors were probably two factors caused the observed discrepancy of PALS and UAVSAR comparisons. The incidence angle of PALS was 40 degrees, while UAVSAR ranged between 25 – 65 degrees and normalized to 40 degrees. Additionally, the original resolution of change in radar backscatter of UAVSAR was at 1.66 – 3 m and aggregated to 1600 m, which was different from the resolution of change in radar backscatter directly measured by PALS instrument at 1600 m.

4.3 DISAGGREGATED CHANGE IN SOIL MOISTURE AT 800 M RESOLUTION USING UAVSAR

The soil moisture sampling was conducted on the days with no rain so there was a total of 17 nonconsecutive days that were sampled between June 7 and July 19. The algorithm was expected to be applicable for disaggregating change in soil moisture within 1-5 days, as the change of vegetation characteristics less than 3 days was not expected to have a significant impact on the relative sensitivity of radar backscatter to soil moisture. According to this rule, we selected five sets of day pairs: June 22 - June 25, July 3 - July 5, July 8 - July 10, July 10 - July 13 and July 14 - July 17, to show the variation of soil moisture during the entire period of the campaign. The disaggregated change in soil moisture at 800 m using UAVSAR observations is shown in Figure 7. A good agreement of the soil moisture spatial distribution patterns can be observed between the original and disaggregated data. Faster changes of soil moisture from -0.4-0.4 m^3/m^3, and both dry-down / wetting trends can be noticed in the southern part of the area than the northern area where the variation is shown in light blue and ranges from -0.2-0.2 m^3/m^3. This fact agrees with the spatial and temporal patterns demonstrated in Figure 4 which are largely determined by land covers. In the southeast part of the study area, the soil moisture varied in response to the precipitation events shown in Figure 2. Modification of soil structure (plowing) and irrigation could be major reasons determining such change trends. In the southern region, the cultural practices by the farmers could change the soil infiltration rate and responded to quicker soil moisture change. And, the irrigated crop fields might also lead to greater soil moisture temporal variabilities than the non-irrigated northern region.

By examining the validation results of the UAVSAR disaggregated soil moisture at 800 m in Figure 8 and Table 3, we can observe that the slope, 95% confidence interval on slope, RMSE, unbiased RMSE all show downgrading tendencies, while R^2 and bias are not significantly affected when the VWC increases. In addition, the overestimation trend of the disaggregated soil moisture can be observed from the slopes.

4.4 DISAGGREGATED UAVSAR SOIL MOISTURE AT 5 M RESOLUTION

Figure 9 a-b shows the aerial photos and UAVSAR disaggregated soil moisture at 5 m for the three sites corresponding to different crop types: canola, soybeans and corn. The man-made structures (buildings, roads, e.g.) in field 62 and 112 shown in Figure 9a lead to abnormally high/low soil moisture values comparing to their surrounding areas covered by crops. And, the soil moisture spatial and temporal variabilities in the crop covered areas observed in Figure 9b did not present in the aerial photos in Figure 9a. A clear wetting trend can be observed for all three sites when comparing Figure 9 with Figure 2 (July 3 – July 5). The observations on July 5 were acquired after a precipitation event, which resulted in a soil moisture change of -0.10-0.03 m^3/m^3. In addition, canola field showed greater spatial and temporal heterogeneity than the other two crop types in the first two images. This might be due to the faster growing of canola and its impact on surface layer soil moisture. From July 13 to July 14, soil moisture dry-down occurred and it was followed by a minor wetting event on July 14-July 17. These precipitation events are consistent with those shown in Figure 2. It also can be observed that the crop canopy row structure (Figure 9b-iii) was reflected in the disaggregated change in soil moisture, with parallel bright strips indicating the increased attenuation of radar signals on the crop canopy. This spatial heterogeneity feature did not present in either canola (Figure 9b-i) or soybeans

(Figure 9b-ii) fields. One possible reason could be that the corn plants were grown in rows and with mature plant structures, which were easier to identify than the other two crop types. The soil moisture variability in the canola field was lower than the other two fields, which was probably due to the presence of uniform vegetation distribution throughout the field. The canola plants were spaced closer to each other and the fraction of field with bare soil was lower.

The validation results for the UAVSAR disaggregated soil moisture at 5 m are shown in Tables 4. The correlation between soil moisture observations and estimates is the lowest for the cornfield ($R^2 = 0.46$) as compared to the other two crop types (0.514-0.79 for soybeans and 0.767 for canola). In addition, the unbiased RMSE ranging between 0.025-0.171 m^3/m^3 also indicates high accuracy of disaggregated soil moisture at 5 m resolution. The possible reason for the R^2 and standard deviation vary between different crop types could be that corn had higher VWC than soybeans and canola, which affected the performance of soil moisture disaggregation. Additionally, the difference in the spatial standard deviation SD between the UAVSAR disaggregated soil moisture and the ground based measurements ΔSD range between <0.001-0.131 m^3/m^3. The soybeans sites 111 and 112, with ΔSD of 0.022 and <0.001 m^3/m^3, respectively, have the best agreement with the *in situ* data. This fact is also reflected in the slopes of fitted lines in Figure 10. SD of the disaggregated results are always greater than the ground based measurements, indicating overestimation of the soil moisture spatial variation. This is probably caused by the uncertainties from two sources: (1) biased prediction of change in soil moisture from the linear regression equations of the change detection algorithm; (2) the inaccuracies from the

original resolution PALS soil moisture retrievals. The overestimation trend corresponds to the Figure 10, where the slopes are mostly over 1.

5 DISCUSSIONS AND CONCLUSIONS

In this paper, a change detection algorithm for disaggregating microwave soil moisture data using aircraft observations was implemented. The passive microwave soil moisture at 1600 m resolution data acquired in SMAPVEX12 campaign was combined with coincident L-band HH polarization radar backscatter coefficient data at resolutions of 5 m and 800 m. The algorithm was developed using the linear relationships between the change in soil moisture and changes in the microwave radiometer and radar measurements, and ignored the impact of any change in the vegetation canopy on the sensitivity of radar backscatter signal to soil moisture over a short period (generally consecutive days).

The PALS soil moisture retrievals and UAVSAR radar data acquisitions during June-July, 2012 were applied to implement the disaggregation algorithm at different spatial resolutions and validated using ground based soil moisture measurements. The validation of PALS radiometer soil moisture retrievals yields R^2 ranging 0.571-0.772, unbiased RMSE ranging 0.025-0.033 m^3/m^3 and bias ranging 0.015-0.033 m^3/m^3. They all indicate good correlation between soil moisture retrievals and *in situ* measurements, and, these values do not vary much while the VWC increases. The validation results of PALS radiometer soil moisture demonstrate its high accuracy for implementing the disaggregation algorithm. The correlations between PALS change in soil moisture and PALS/aggregated UAVSAR change in backscatter are fairly good, with R^2 of 0.68-0.77

and 0.6-0.76, respectively. This proves the aforementioned assumption of the linear relationship between them. The results show that the disaggregated change in soil moisture for UAVSAR is well correlated to the *in situ* soil moisture measurements, with R^2 ranging 0.628-0.794 and unbiased RMSE ranging 0.025-0.091 m^3/m^3. The validation variables for disaggregated UAVSAR soil moistures have similar ranges as these of the PALS radiometer soil moistures. The variables for the disaggregated UAVSAR do not significantly degrade as the VWC < 2.5 kg/m^2, which agrees with the assumption that the vegetation characteristics of the radar pixels can be summarized by the corresponding radiometer pixel which they fall in. However, it could be noted that the VWC between 2-2.5 kg/m^2 shows greater uncertainties, indicating the heavy vegetation coverage may lead to downgrading of estimated soil moistures. In addition, the UAVSAR disaggregated change in soil moisture is overestimated for all VWC groups when compared with the ground based data. This trend may be due to (1) the fact that point-based ground measurements are not representative of soil moisture pixel; (2) the quality of PALS radiometer soil moisture retrievals; and (3) the sensing depth difference between radar soil moisture and ground measurements. It is also noted that the aggregated UAVSAR radar backscatter at 1600 m has a good correlation when VWC <6 kg/m^2, with R^2 ranging 0.642-0.777. This suggests that the change detection algorithm can disaggregate the PALS change in soil moisture by using the UAVSAR change in radar backscatter. Furthermore, the disaggregation method was also applied with the 5 m resolution UAVSAR radar data in order to examine higher resolution soil moisture spatial variability within one crop field. These changes in the soil moisture maps at 5 m show the greater spatial heterogeneity of soil moisture. The overestimation tendency is also observed in the validation results, with

the difference of spatial standard deviation ranging from <0.001-0.131 m^3/m^3. Examining the other validation metrics, the overall R^2 (0.46-0.79), unbiased RMSE (0.025-0.171 m^3/m^3) and bias (-0.168-0.008 m^3/m^3) do not show a significant difference between different crop types.

Comparing with previous publications that mentioned the RMSE of their disaggregated soil moisture estimates, such as Narayan et al., 2006 with RMSE range of 0.02-0.03 m^3/m^3; Merlin et al., 2009 with an average RMSE of -0.062 m^3/m^3, Piles et al., 2011 with RMSE range of 0.09-0.17 m^3/m^3, the disaggregated soil moisture errors reported here are at the same level of accuracy as these investigations. Another contributing factor is that the algorithm proposed here is applied to disaggregating 1600 m resolution soil moisture to 5 m / 800 m resolution, which has a greater cross scale of spatial resolution than the other algorithms. Therefore, more uncertainties may be introduced in the disaggregation implementation.

The major limitation of this disaggregation algorithm is the assumption that within the radiometer pixel, the spatial variability of soil roughness and vegetation canopy parameters to the spatial variability of radar signal sensitivity can be ignored. This assumption can be applied at field scale region with uniform vegetation coverage and low vegetation opacity within a short period of 2-3 days. However, these conditions are often oversimplified for the thicker canopy vegetation or long-term soil moisture estimation. Future study will aim to model the relationship between vegetation parameters and radar sensitivity of canopy. This algorithm should also account for vegetation variability at subpixel level within radiometer pixel. Moreover, future study will apply the change

detection algorithm method to estimate change in soil moisture from the other airborne remote sensing products.

Currently, the radar soil moisture retrieval algorithms are restricted to calculate absolute soil moisture from radar backscatter observations, because the algorithms require to input ancillary data of high spatial resolution, including surface soil roughness, vegetation canopy parameters. And, the algorithms work only under low vegetation water conditions (Jackson et al., 1996; Oh et al., 1992; Dubois et al., 1995). As opposed to this, the change detection algorithm does not require the soil and vegetation parameters and assumes their influence could be ignored at a very short period. The study presented here proposed a simple approach to estimate high spatial resolution of soil moisture temporal change from microwave radiometer retrievals by only using radiometer observations and radar backscatter coefficients without requiring ancillary data sets. This study can be potentially applied to estimate soil moisture for agricultural and hydrological studies once simultaneous passive microwave soil moisture retrievals and high spatial resolution active microwave observations are available.

6 ACKNOWLEDGEMENTS

The SMAPVEX12 UAVSAR and *in situ* data are provided by National Snow and Ice Data Center (NSIDC) at http://nsidc.org/data. This work was funded by the NASA Terrestrial Hydrology Program (Program Manager Dr. Jared Entin).

REFERENCES

Bindlish, R., and Barros, A. P. (2002). Subpixel variability of remotely sensed soil moisture: An inter-comparison study of SAR and ESTAR. *IEEE Transactions on Geoscience and Remote Sensing*, *40*(2), 326-337.

Bolten, J. D., Lakshmi, V., and Njoku, E. G. (2003). Soil moisture retrieval using the passive/active L-and S-band radar/radiometer. *IEEE Transactions on Geoscience and Remote Sensing*, *41*(12), 2792-2801.

Carlson, T. N., Gillies, R. R., and Schmugge, T. J. (1995). An interpretation of methodologies for indirect measurement of soil water content. *Agricultural and forest meteorology*, *77*(3-4), 191-205.

Carlson, T. (2007), An overview of the "triangle method" for estimating surface evapo-transpiration and soil moisture from satellite imagery, *Sensors, 7*, 1612–1629.

Choi, M., and Hur, Y. (2012). A microwave-optical/infrared disaggregation for improving spatial representation of soil moisture using AMSR-E and MODIS products. *Remote Sensing of Environment*, *124*, 259-269.

Choudhury, B. J., Schmugge, T. J., Chang, A., and Newton, R. W. (1979). Effect of surface roughness on the microwave emission from soils. *Journal of Geophysical Research: Oceans (1978–2012), 84*(C9), 5699-5706.

Colliander, A. (2013a). SMAPVEX12 PALS Brightness Temperature Data. Boulder, Colorado USA: NASA DAAC at the National Snow and Ice Data Center.

Colliander, A. (2013b). SMAPVEX12 PALS Backscatter Data. Boulder, Colorado USA: NASA DAAC at the National Snow and Ice Data Center.

Colliander, A., Jackson, T., McNairn, H., Chazanoff, S., Dinardo, S., Latham, B., ... and Njoku, E. (2015). Comparison of airborne passive and active L-band system (PALS) brightness temperature measurements to SMOS observations during the SMAP validation experiment 2012 (SMAPVEX12). *IEEE Geoscience and Remote Sensing Letters*, *12*(4), 801-805.

Colliander, A., Njoku, E. G., Jackson, T. J., Chazanoff, S., McNairn, H., Powers, J., and Cosh, M. H. (2016). Retrieving soil moisture for non-forested areas using PALS radiometer measurements in SMAPVEX12 field campaign. Remote Sensing of Environment, 184, 86-100.

Cosh, M. (2015). SMAPVEX12 Vegetation Water Content Map. Boulder, Colorado USA: NASA National Snow and Ice Data Center Distributed Active Archive Center.

Cosh, M. H., Jackson, T. J., Bindlish, R., and Prueger, J. H. (2004). Watershed scale

temporal and spatial stability of soil moisture and its role in validating satellite estimates. *Remote sensing of Environment, 92*(4), 427-435.

Das, N. N., Entekhabi, D., and Njoku, E. G. (2011). An algorithm for merging SMAP radiometer and radar data for high-resolution soil-moisture retrieval. *Geoscience and Remote Sensing, IEEE Transactions on, 49*(5), 1504-1512.

Du, Y., Ulaby, F. T., and Dobson, M. C. (2000). Sensitivity to soil moisture by active and passive microwave sensors. *Geoscience and Remote Sensing, IEEE Transactions on, 38*(1), 105-114.

Dubois, P. C., Van Zyl, J., and Engman, T. (1995). Measuring soil moisture with imaging radars. *IEEE Transactions on Geoscience and Remote Sensing*, *33*(4), 915-926.

Engman, E. T., and Chauhan, N. (1995). Status of microwave soil moisture measurements with remote sensing. *Remote Sensing of Environment, 51*(1), 189-198.

Entekhabi, D., Njoku, E. G., O'Neill, P. E., Kellogg, K. H., Crow, W. T., Edelstein, W. N., ... and Van Zyl, J. (2010). The soil moisture active passive (SMAP) mission. *Proceedings of the IEEE, 98*(5), 704-716.

Fang, B., Lakshmi, V., Bindlish, R., Jackson, T. J., Cosh, M., and Basara, J. (2013). Passive microwave soil moisture downscaling using vegetation index and skin surface temperature. *Vadose Zone Journal, 12*(3).

Fang, B., and Lakshmi, V. (2014a). Soil moisture at watershed scale: Remote sensing techniques. *Journal of Hydrology, 516*, 258-272.

Fang, B., and Lakshmi, V. (2014b). AMSR-E Soil Moisture Disaggregation Using MODIS and NLDAS Data. *Remote Sensing of the Terrestrial Water Cycle*, 277-304, Published by John Wiley.

Fang, B., Lakshmi, V., Bindlish, R., and Jackson, T. J. (2018a). Downscaling of SMAP soil moisture using land surface temperature and vegetation data. *Vadose Zone Journal*, *17*(1).

Fang, B., Lakshmi, V., Bindlish, R., and Jackson, T. (2018b). AMSR2 Soil Moisture Downscaling Using Temperature and Vegetation Data. *Remote Sensing*, *10*(10), 1575.

Fung, A. K., Li, Z., and Chen, K. S. (1992). Backscattering from a randomly rough dielectric surface. *Geoscience and Remote Sensing, IEEE Transactions on, 30*(2), 356-369.

Gillies, R. R., and Carlson, T. N. (1995). Thermal remote sensing of surface soil water content with partial vegetation cover for incorporation into climate models. *Journal of Applied Meteorology, 34*(4), 745-756.

Heathman, G. C., Cosh, M. H., Han, E., Jackson, T. J., McKee, L., and McAfee, S. (2012). Field scale spatiotemporal analysis of surface soil moisture for evaluating point-scale in situ networks. *Geoderma, 170*, 195-205.

Jackson, T. J., and Schmugge, T. J. (1989). Passive microwave remote sensing system for soil moisture: Some supporting research. *Geoscience and Remote Sensing, IEEE Transactions on, 27*(2), 225-235.

Jackson, T. J. (1993). III. Measuring surface soil moisture using passive microwave remote sensing. *Hydrological processes, 7*(2), 139-152.

Jackson, T. J., Schmugge, J., and Engman, E. T. (1996). Remote sensing applications to hydrology: soil moisture. *Hydrological Sciences Journal*, *41*(4), 517-530.

Jackson, T. J., Le Vine, D. M., Hsu, A. Y., Oldak, A., Starks, P. J., Swift, C. T., ... and Haken, M. (1999). Soil moisture mapping at regional scales using microwave radiometry: The Southern Great Plains Hydrology Experiment. *Geoscience and Remote Sensing, IEEE Transactions on, 37*(5), 2136-2151.

Jackson, T. J., Gasiewski, A. J., Oldak, A., Klein, M., Njoku, E. G., Yevgrafov, A., ... and Bindlish, R. (2002). Soil moisture retrieval using the C-band polarimetric scanning radiometer during the Southern Great Plains 1999 Experiment. *Geoscience and Remote Sensing, IEEE Transactions on, 40*(10), 2151-2161.

Jackson, T. J., Cosh, M. H., Bindlish, R., Starks, P. J., Bosch, D. D., Seyfried, M., ... and Du, J. (2010). Validation of advanced microwave scanning radiometer soil moisture products. *Geoscience and Remote Sensing, IEEE Transactions on, 48*(12), 4256-4272.

Jackson, T. J., Bindlish, R., Cosh, M. H., Zhao, T., Starks, P. J., Bosch, D. D., ... and Leroux, D. (2012). Validation of soil moisture and ocean salinity (SMOS) soil moisture over watershed networks in the US. *Geoscience and Remote Sensing, IEEE Transactions on, 50*(5), 1530-1543.

Kerr, Y. H., Waldteufel, P., Richaume, P., Davenport, I., Ferrazzoli, P., and Wigneron, J. P. (2007). SMOS Level 2 Processor for Soil Moisture, Algorithm Theoretical Based Document (ATBD). *CESBIO, IPSL-Service d'Aéronomie, INRAEPHYSE*, Reading University, Tor Vergata University. SO-TN-ESL-SM-GS-0001 Issue 3. a, 05/12/2007.

Kim, J., and Hogue, T. S. (2012). Improving spatial soil moisture representation through integration of AMSR-E and MODIS products. *Geoscience and Remote Sensing, IEEE Transactions on, 50*(2), 446-460.

Kim, S.B., T.J. Jackson, S.H. Yueh, X. Xu, and S. Hensley, Feasibility of inter-comparing airborne and spaceborne observations of radar backscattering coefficients for soil moisture retrieval. (2015) *J. Selected Topics Applied Earth Obs. Rem. Sens. In Press*.

Lakshmi, V., Wood, E. F., and Choudhury, B. J. (1997). Evaluation of Special Sensor Microwave/Imager satellite data for regional soil moisture estimation over the Red River Basin. *Journal of Applied Meteorology, 36*(10), 1309-1328.

Lakshmi, V. (2004). The role of satellite remote sensing in the prediction of ungauged basins. *Hydrological processes, 18*(5), 1029-1034.

Lakshmi, V., Hong, S., Small, E. E., and Chen, F. (2011). The influence of the land surface on hydrometeorology and ecology: new advances from modeling and satellite remote sensing. *Hydrology Research, 42*(2-3), 95-112.

Lakshmi, V. (2013). Remote sensing of soil moisture. *ISRN Soil Science*, 2013.

Land Long Term Data Record (LTDR). AVHRR data. http://ltdr.nascom.nasa.gov/

Luo, Y., Berbery, E. H., Mitchell, K. E., and Betts, A. K. (2007). Relationships between land surface and near-surface atmospheric variables in the NCEP North American Regional Reanalysis. *Journal of Hydrometeorology, 8*(6), 1184-1203.

Mallick, K., Bhattacharya, B. K., and Patel, N. K. (2009). Estimating volumetric surface moisture content for cropped soils using a soil wetness index based on surface temperature and NDVI. Agricultural and Forest Meteorology, 149(8), 1327-1342.

McNairn, H., Jackson, T. J., Wiseman, G., Belair, S., Berg, A., Bullock, P., ... and Moghaddam, M. (2015). The Soil Moisture Active Passive Validation Experiment 2012 (SMAPVEX12): Prelaunch calibration and validation of the SMAP soil moisture algorithms. *IEEE Transactions on Geoscience and Remote Sensing*, *53*(5), 2784-2801.

Merlin, O., Chehbouni, A., Walker, J. P., Panciera, R., and Kerr, Y. H. (2008). A simple method to disaggregate passive microwave-based soil moisture. *Geoscience and Remote Sensing, IEEE Transactions on, 46*(3), 786-796.

Merlin, O., Walker, J. P., Chehbouni, A., and Kerr, Y. (2008). Towards deterministic downscaling of SMOS soil moisture using MODIS derived soil evaporative efficiency. *Remote Sensing of Environment, 112*(10), 3935-3946.

Merlin, O., Al Bitar, A., Walker, J. P., and Kerr, Y. (2009). A sequential model for disaggregating near-surface soil moisture observations using multi-resolution thermal sensors. *Remote Sensing of Environment, 113*(10), 2275-2284.

Merlin, O., Al Bitar, A., Walker, J. P., and Kerr, Y. (2010). An improved algorithm for disaggregating microwave-derived soil moisture based on red, near-infrared and thermal-infrared data. *Remote Sensing of Environment, 114*(10), 2305-2316.

Merlin, O., Rudiger, C., Al Bitar, A., Richaume, P., Walker, J. P., and Kerr, Y. H.

(2012). Disaggregation of SMOS soil moisture in Southeastern Australia. *Geoscience and Remote Sensing, IEEE Transactions on, 50*(5), 1556-1571.

Merlin, O., Escorihuela, M. J., Mayoral, M. A., Hagolle, O., Al Bitar, A., and Kerr, Y. (2013). Self-calibrated evaporation-based disaggregation of SMOS soil moisture: An evaluation study at 3km and 100m resolution in Catalunya, Spain. *Remote Sensing of Environment, 130*, 25-38.

Minacapilli, M., Iovino, M., and Blanda, F. (2009). High resolution remote estimation of soil surface water content by a thermal inertia approach. *Journal of hydrology, 379*(3), 229-238.

Minet, J., Bogaert, P., Vanclooster, M., and Lambot, S. (2012). Validation of ground penetrating radar full-waveform inversion for field scale soil moisture mapping. *Journal of Hydrology, 424*, 112-123.

Mladenova, I., Lakshmi, V., Walker, J. P., Panciera, R., Wagner, W., and Doubkova, M. (2010). Validation of the ASAR global monitoring mode soil moisture product using the NAFE'05 data set. *Geoscience and Remote Sensing, IEEE Transactions on, 48*(6), 2498-2508.

Mladenova, I., Lakshmi, V., Jackson, T. J., Walker, J. P., Merlin, O., and de Jeu, R. A. (2011). Validation of AMSR-E soil moisture using L-band airborne radiometer data from National Airborne Field Experiment 2006. *Remote Sensing of Environment, 115*(8), 2096-2103.

Mohanty, B. P., Famiglietti, J. S., and Skaggs, T. H. (2000). Evolution of soil moisture spatial structure in a mixed vegetation pixel during the Southern Great Plains 1997 (SGP97) Hydrology Experiment. *Water Resources Research, 36(12)*, 3675-3686.

Narayan, U., Lakshmi, V., and Jackson, T. J. (2006). High-resolution change estimation of soil moisture using L-band radiometer and radar observations made during the SMEX02 experiments. *Geoscience and Remote Sensing, IEEE Transactions on, 44(6)*, 1545-1554.

Narayan, U., and Lakshmi, V. (2008). Characterizing subpixel variability of low resolution radiometer derived soil moisture using high resolution radar data. *Water resources research, 44*(6).

Niu, C. Y., Musa, A., and Liu, Y. (2015). Analysis of soil moisture condition under different land uses in the arid region of Horqin sandy land, northern China. *Solid Earth*, *6*(4), 1157-1167.

Njoku, E. G., and Entekhabi, D. (1996). Passive microwave remote sensing of soil moisture. *Journal of hydrology, 184*(1), 101-129.

Njoku, E. G., and Li, L. (1999). Retrieval of land surface parameters using passive microwave measurements at 6-18 GHz. *Geoscience and Remote Sensing, IEEE Transactions on, 37*(1), 79-93.

Njoku, E. G., Wilson, W. J., Yueh, S. H., Dinardo, S. J., Li, F. K., Jackson, T. J., ... and Bolten, J. (2002). Observations of soil moisture using a passive and active low-frequency microwave airborne sensor during SGP99. *IEEE Transactions on Geoscience and Remote Sensing*, *40*(12), 2659-2673.

Njoku, E. G., Jackson, T. J., Lakshmi, V., Chan, T. K., and Nghiem, S. V. (2003). Soil moisture retrieval from AMSR-E. *Geoscience and Remote Sensing, IEEE Transactions on, 41*(2), 215-229.

Njoku, E. G., and Chan, S. K. (2006). Vegetation and surface roughness effects on AMSR-E land observations. *Remote Sensing of environment, 100*(2), 190-199.

Oh, Y., Sarabandi, K., and Ulaby, F. T. (1992). An empirical model and an inversion technique for radar scattering from bare soil surfaces. *IEEE transactions on Geoscience and Remote Sensing*, *30*(2), 370-381.

Pan, M., Wood, E. F., McLaughlin, D. B., Entekhabi, D., and Luo, L. (2009). A multiscale ensemble filtering system for hydrologic data assimilation. Part I: Implementation and synthetic experiment. *Journal of Hydrometeorology*, *10*(3), 794-806.

Parada, L. M., and Liang, X. (2004). Optimal multiscale Kalman filter for assimilation of near-surface soil moisture into land surface models. *Journal of Geophysical Research: Atmospheres (1984–2012), 109*(D24).

Peischl, S., Walker, J. P., Allahmoradi, M., Barrett, D., Gurney, R., Kerr, Y., ... and Ye, N. (2009, July). Towards validation of SMOS using airborne and ground data over the Murrumbidgee Catchment. In *Proc. MODSIM* (pp. 3733-3739).

Peng, J., Loew, A., Merlin, O., and Verhoest, N. E. (2017). A review of spatial downscaling of satellite remotely sensed soil moisture. *Reviews of Geophysics*, *55*(2), 341-366.

Piles, M., Entekhabi, D., and Camps, A. (2009). A change detection algorithm for retrieving high-resolution soil moisture from SMAP radar and radiometer observations. *Geoscience and Remote Sensing, IEEE Transactions on, 47*(12), 4125-4131.

Piles, M., Camps, A., Vall-Llossera, M., Corbella, I., Panciera, R., Rudiger, C., ... and Walker, J. (2011). Downscaling SMOS-derived soil moisture using MODIS visible/infrared data. *Geoscience and Remote Sensing, IEEE Transactions on, 49*(9), 3156-3166.

Rodríguez-Iturbe, I., G. K. Vogel, R. Rigon, D. Entekhabi, F. Castelli, and A.Rinaldo (1995), On the Spatial Organization of Soil Moisture Fields, *Geophysical Research Letters, 22*(20), 2757-2760.

Sánchez-Ruiz, S., Piles, M., Sánchez, N., Martínez-Fernández, J., Vall-llossera, M., and Camps, A. (2014). Combining SMOS with visible and near/shortwave/thermal infrared satellite data for high resolution soil moisture estimates. *Journal of Hydrology, 516*, 273-283.

Sahoo, A. K., De Lannoy, G. J., Reichle, R. H., and Houser, P. R. (2013). Assimilation and downscaling of satellite observed soil moisture over the Little River Experimental Watershed in Georgia, USA. *Advances in Water Resources, 52*, 19-33.

Schmugge, T., Gloersen, P., Wilheit, T., and Geiger, F. (1974). Remote sensing of soil moisture with microwave radiometers. *Journal of Geophysical Research, 79*(2), 317-323.

Schmugge, T., and Jackson, T. J. (1994). Mapping surface soil moisture with microwave radiometers. *Meteorology and Atmospheric Physics, 54*(1-4), 213-223.

Schmugge, T. J., Kustas, W. P., Ritchie, J. C., Jackson, T. J., and Rango, A. (2002). Remote sensing in hydrology. *Advances in water resources, 25*(8), 1367-1385.

Wigneron, J. P., Chanzy, A., Calvet, J. C., and Bruguier, N. (1995). A simple algorithm to retrieve soil moisture and vegetation biomass using passive microwave measurements over crop fields. *Remote Sensing of Environment, 51*(3), 331-341.

Wiseman, G., A. Berg, and P. Bullock. (2014). SMAPVEX12 Probe-Based In Situ Soil Moisture Data for Agricultural Area. Boulder, Colorado USA: NASA National Snow and Ice Data Center Distributed Active Archive Center.

Xu, Xiaolan. (2014). SMAPVEX12 UAVSAR Incidence-Angle Normalized Backscatter Data. Boulder, Colorado USA: NASA DAAC at the National Snow and Ice Data Center. http://dx.doi.org/10.5067/1A09OKL9G4QW.

Yu, G., Di, L., and Yang, W. (2008, July). Downscaling of global soil moisture using auxiliary data. In *Geoscience and Remote Sensing Symposium, 2008. IGARSS 2008. IEEE International* (Vol. 3, pp. III-230). IEEE.

Zhao, W., and Li, A. (2013). A Downscaling Method for Improving the Spatial Resolution of AMSR-E Derived Soil Moisture Product Based on MSG-SEVIRI Data. *Remote Sensing, 5*(12), 6790-6811.

Zucco, G., Brocca, L., Moramarco, T., and Morbidelli, R. (2014). Influence of land use on soil moisture spatial–temporal variability and monitoring. *Journal of hydrology*, *516*, 193-199.

TABLES AND FIGURES

Table 1 Remote sensing and ground based data sets used in soil moisture disaggregation.

Dataset	Spatial Resolution	Temporal Resolution
PALS L-band (H-pol) Radiometer Brightness Temperature (K)	1600 m (Along Track)	Daily
PALS L-band (HH-pol) Radar Backscatter (dB)	1600 m (Along Track)	Daily
UAVSAR Radar Backscatter (dB)	5 m	Daily
Vegetation Water Content Map (kg/m^2)	5 m	Daily
In situ Soil Moisture observations (m^3/m^3)	800 m	Daily

Table 2 PALS radiometer soil moisture retrievals compared with *in situ* soil moisture measurements from June 15, June 22, July 13, July 14 and July 19.

VWC	Number of Points	R^2	Slope	95% Confidence Intervals (Slope)	RMSE (m^3/m^3)	Unbiased RMSE (m^3/m^3)	Bias (m^3/m^3)
0<VWC<1.5	49	0.615	0.972	(0.793, 0.944)	0.069	0.032	0.033
1.5<VWC<2	64	0.726	0.887	(0.847, 0.958)	0.066	0.027	0.023
2<VWC<2.5	32	0.772	1.192	(0.862, 1.086)	0.069	0.025	0.015
VWC>2.5	58	0.571	0.818	(0.756, 0.922)	0.072	0.033	0.028

Table 3 Disaggregated UAVSAR change in soil moisture at 800 m resolution validated by *in situ* soil moisture measurements for June 22 - June 25, July 3 - July 5, July 5 - July 8, July 8 - July 10, Jul 10 - July 13.

VWC	Number of Points	R^2	Slope	95% Confidence Intervals (Slope)	RMSE (m^3/m^3)	Unbiased RMSE (m^3/m^3)	Bias (m^3/m^3)
0<VWC<1.5	60	0.667	1.542	(1.28, 1.835)	0.079	0.037	0.012
1.5<VWC<2	22	0.628	1.257	(0.804, 1.664)	0.096	0.025	0.005
2<VWC<2.5	27	0.641	2.257	(1.67, 3.006)	0.141	0.091	0.042
VWC>2.5	40	0.794	1.89	(1.538, 2.152)	0.072	0.049	-0.002

Table 4 Statistical variables R^2, slope, RMSE, unbiased RMSE, bias, spatial standard deviation as well as the difference of spatial standard deviation between UAVSAR and *in situ* data for the disaggregated UAVSAR change in soil moisture at 5 m resolution validated using *in situ* moisture measurements from July 3 - July 5, July 5 - July 8, July 8 - July 10, Jul 10 - July 13.

Site	Type	Number	R^2	Slope	RMSE (m^3/m^3)	Unbiased RMSE (m^3/m^3)	Bias (m^3/m^3)	SD (m^3/m^3)	ΔSD (m^3/m^3)
Site-14	Soybeans	22	0.514	1.171	0.186	0.171	-0.168	0.113	0.064
Site-62	Canola	31	0.767	1.471	0.058	0.044	-0.038	0.081	0.029
Site-63	Soybeans	32	0.79	1.24	0.044	0.035	-0.032	0.061	0.012
Site-71	Corn	51	0.46	2.82	0.145	0.075	0.008	0.169	0.131
Site-111	Soybeans	64	0.676	0.998	0.077	0.027	-0.027	0.128	0.022
Site-112	Soybeans	32	0.739	0.802	0.04	0.025	-0.02	0.062	<0.001

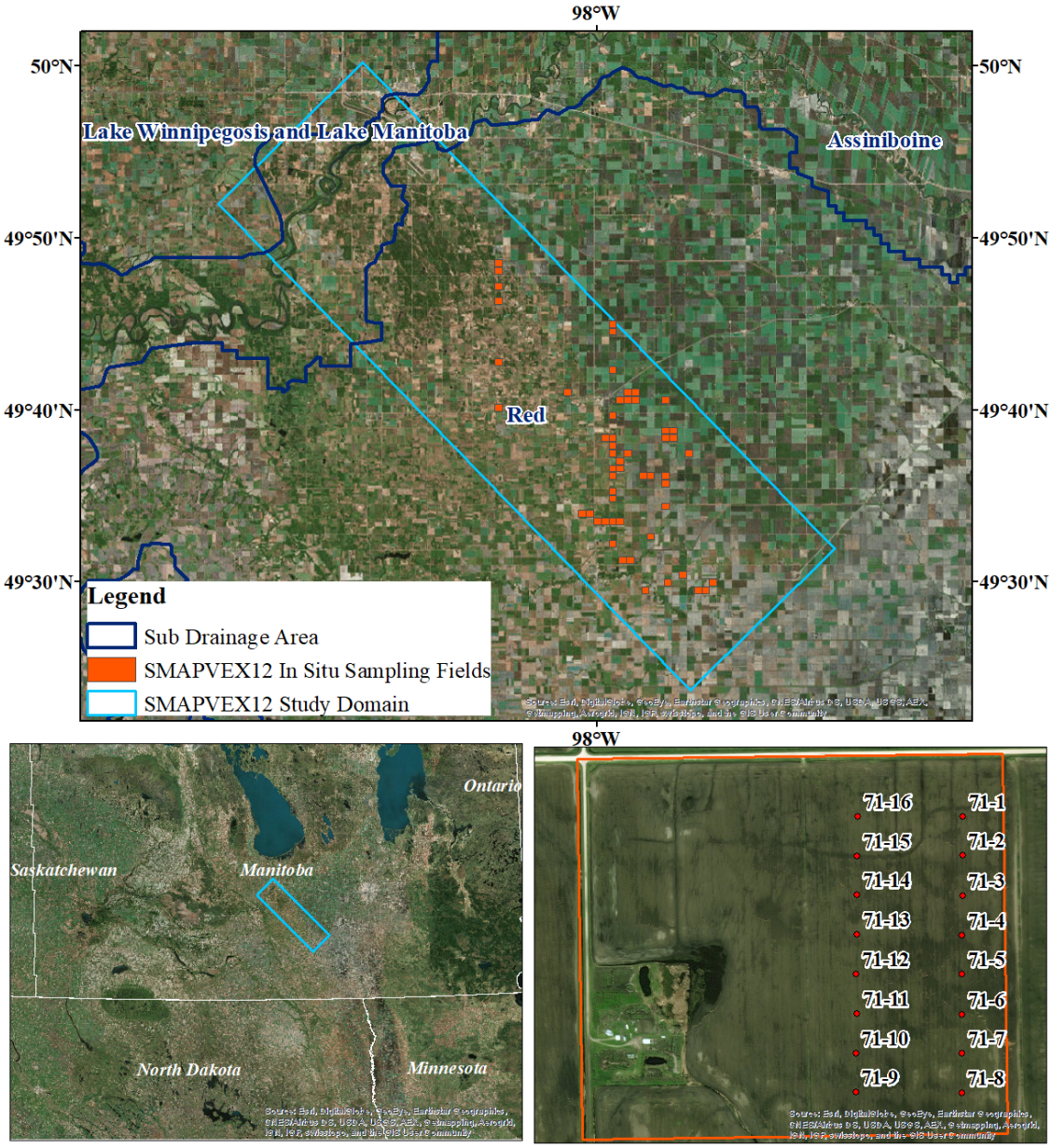

Figure 1. Overview of the SMAPVEX12 study area. The orange color boxes represent sampling fields, including agricultural fields and permanent AAFC (Agriculture and Agri-Food Canada) fields. Lower right graph is a close view of crop field site-71. The ground soil moisture was sampled from 16 points of two parallel rows.

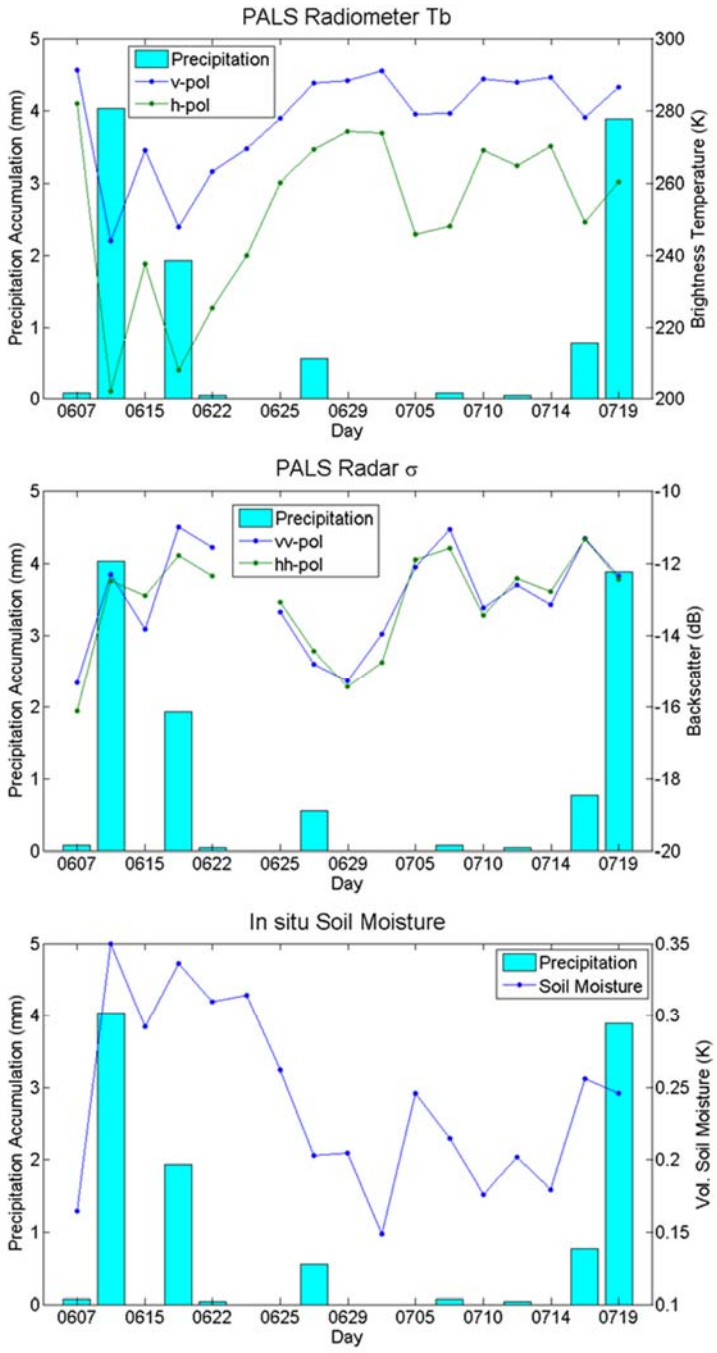

Figure 2. Daily averaged PALS radiometer (high altitude) brightness temperature / radar backscatter data at L-band, ground soil moisture measurements and daily-accumulated precipitation of study area from June 7 - July 19, 2012. The precipitation comes from rain gauges of the Canada WeatherFarm weather station network.

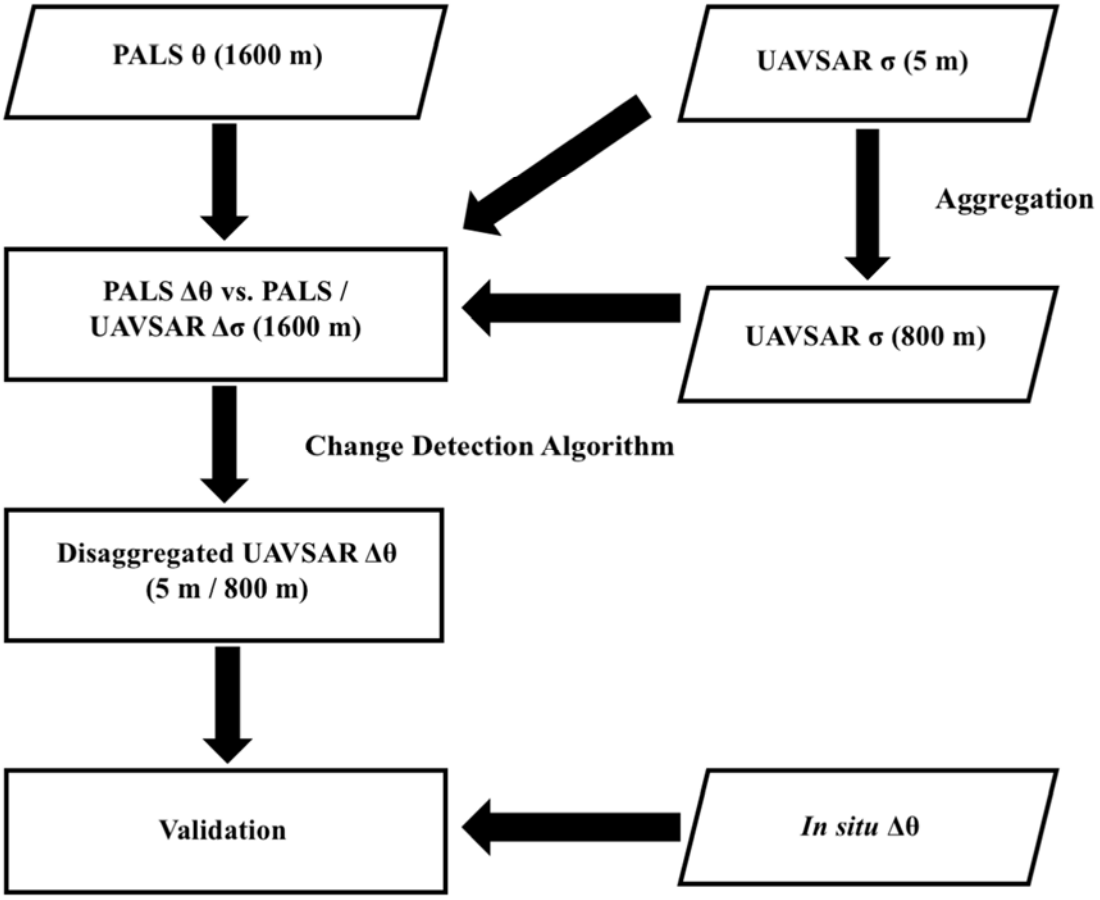

Figure 3. Data flow of the PALS soil moisture disaggregation algorithm.

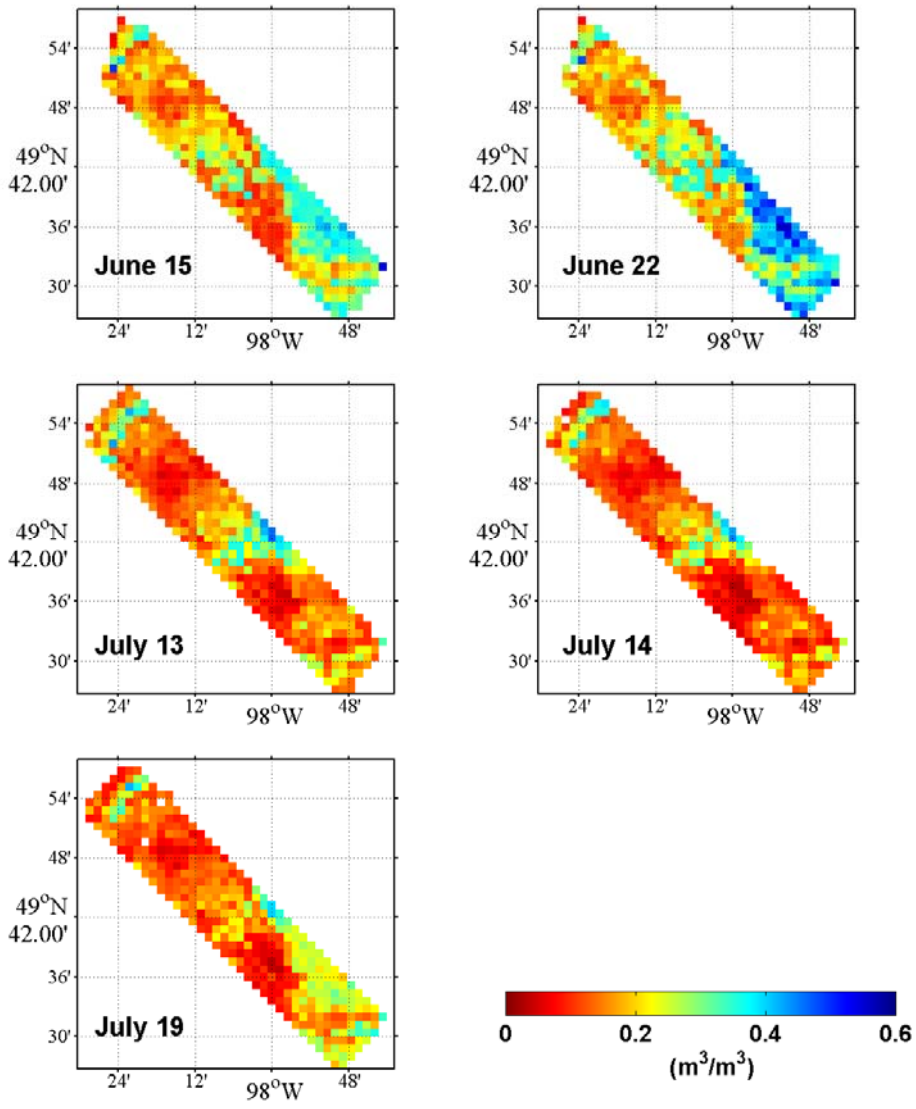

Figure 4. PALS radiometer soil moisture retrievals (m^3/m^3) at 1600 m resolution for five days: June 15, June 22, July 13, July 14 and July 19.

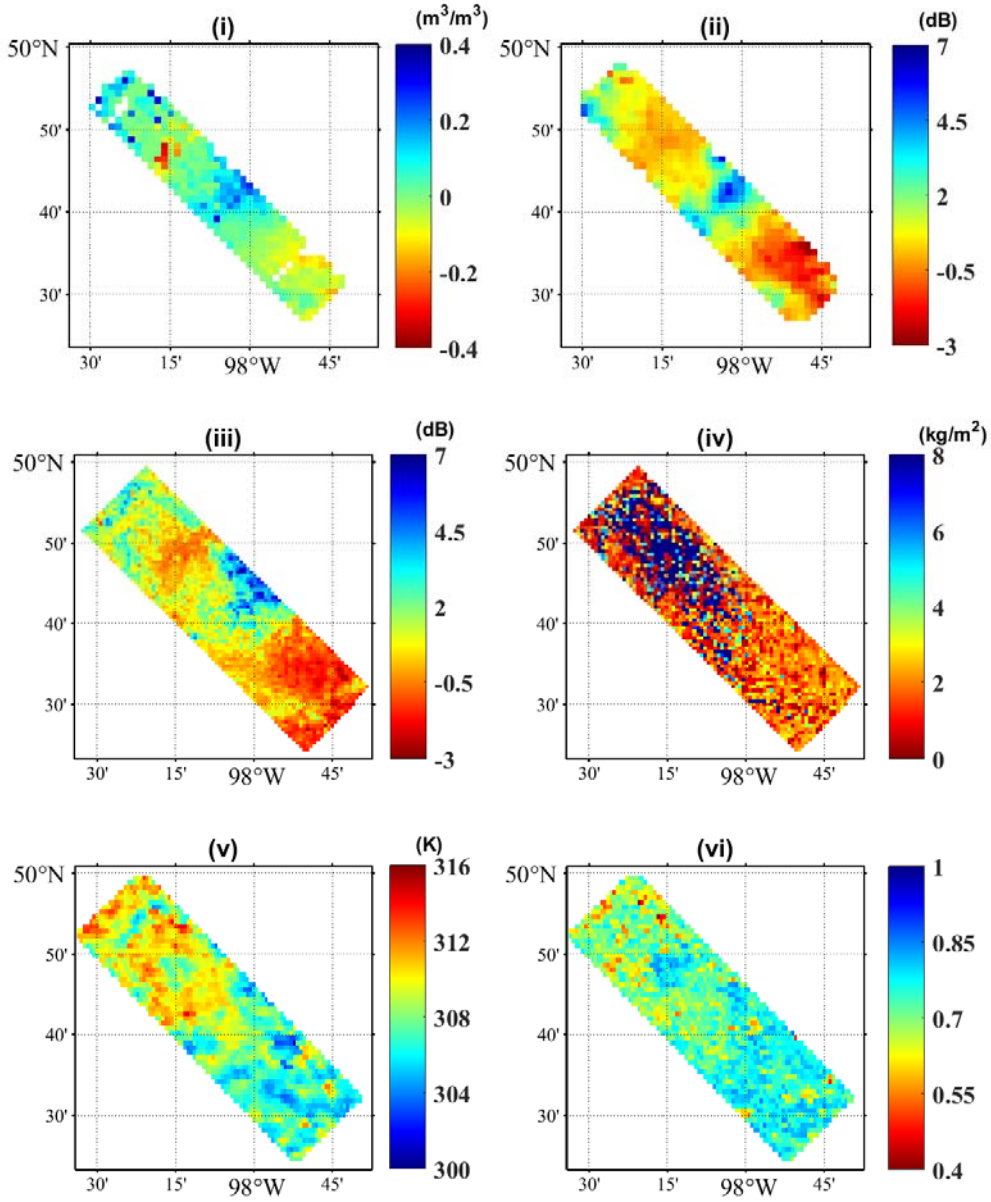

Figure 5. Data sets used in the soil moisture disaggregation study and other related land surface variables from July 10 - July 13: (i) PALS radiometer change in soil moisture (h polarization) retrieval at 1600 m resolution (m^3/m^3); (ii) PALS change in radar backscatter (HH polarization) at 1600 m resolution (dB); (iii) UAVSAR change in radar backscatter (HH polarization) at 800 m resolution; (iv) VWC at 800 m resolution (kg/m^2); (v) MODIS LST at 1000 m resolution (K); (vi) MODIS NDVI at 1000 m resolution.

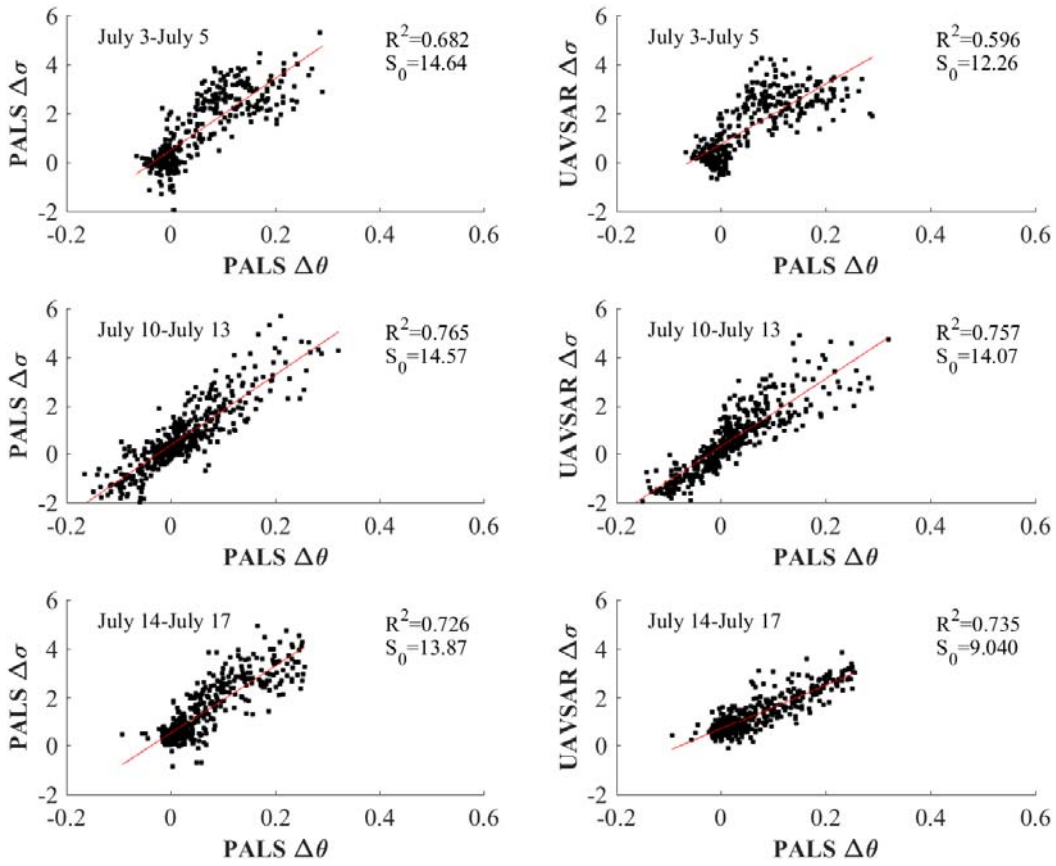

Figure 6. PALS and aggregated UAVSAR radar backscatter at 1600 m resolution compared with PALS radiometer soil moisture retrievals for July 3 - July 5, July 10 - July 13 and July 14 - July 17.

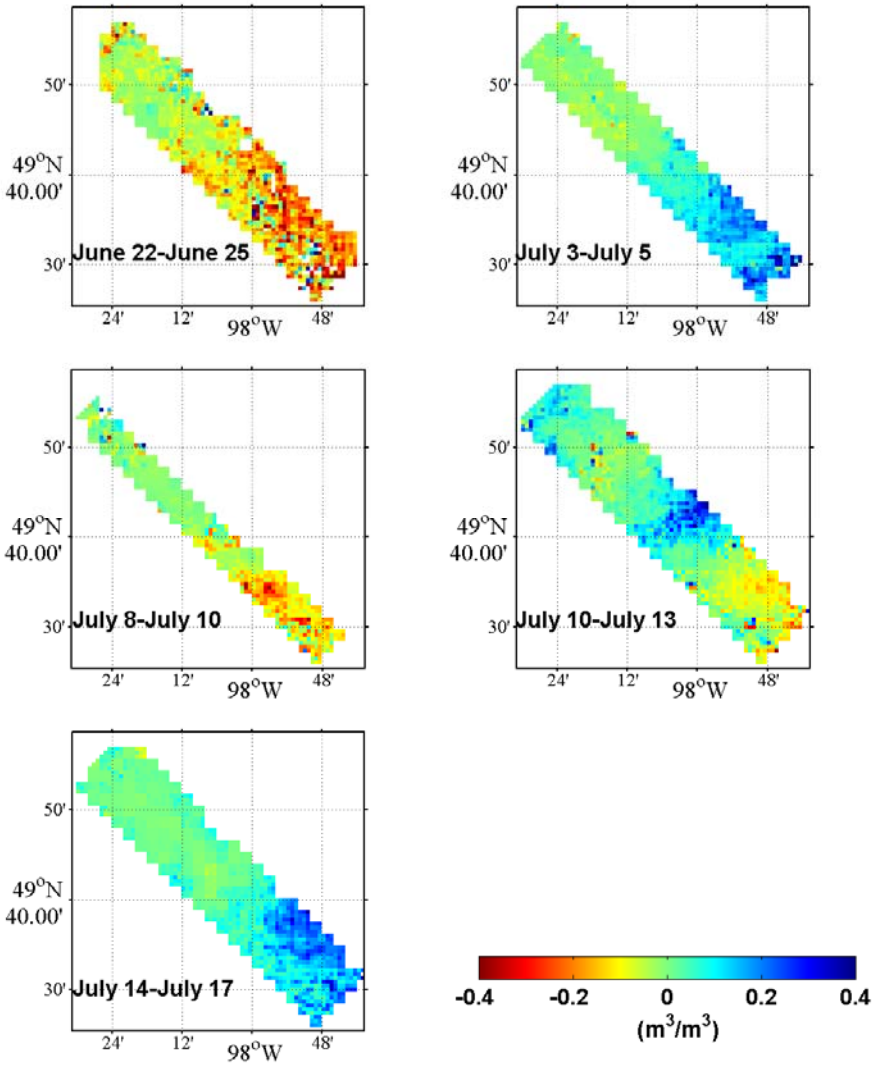

Figure 7. Disaggregated UAVSAR change in soil moisture (m^3/m^3) at 800 m resolution for June 22 - June 25, July 3 - July 5, July 8 - July 10, July 10 - July 13, July 14 - July 17.

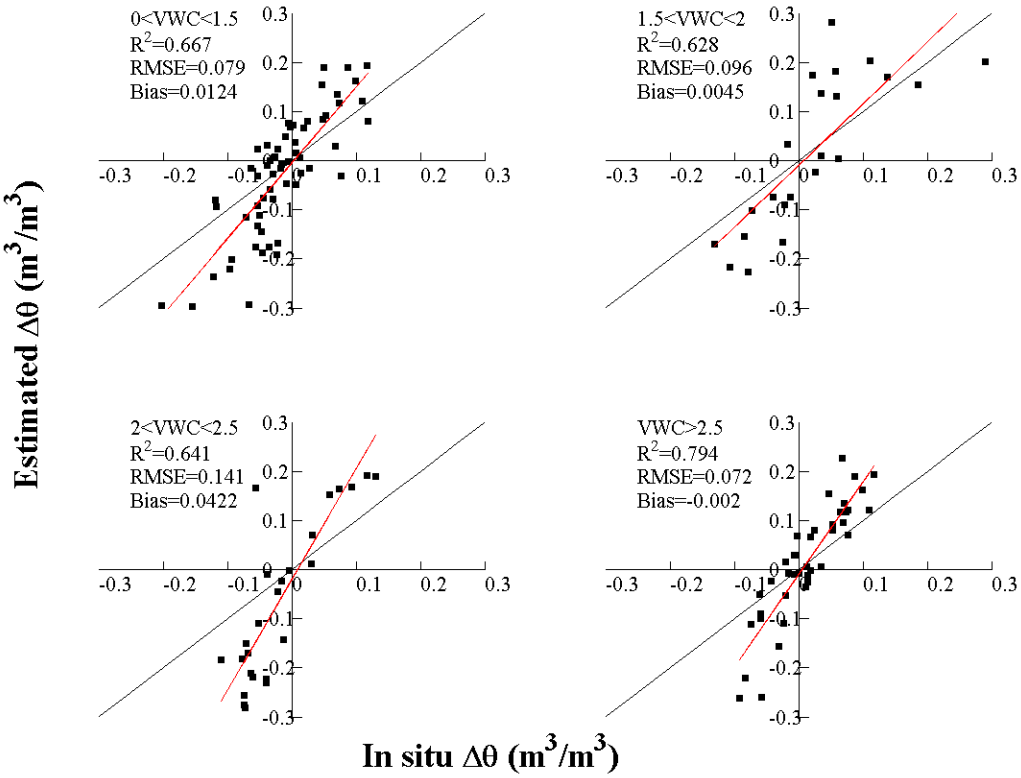

Figure 8. Validation of disaggregated UAVSAR change in soil moisture at 800 m resolution for June 22 - June 25, July 3 - July 5, July 5 - July 8, July 8 - July 10, July 10 - July 13, corresponding to four VWC groups.

Field 62

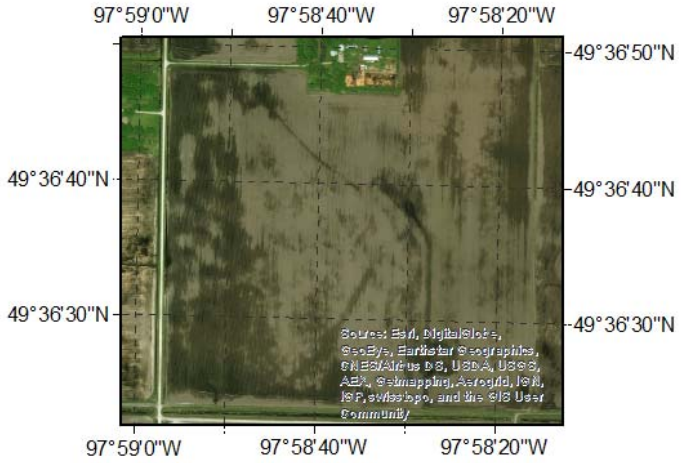

Field 112

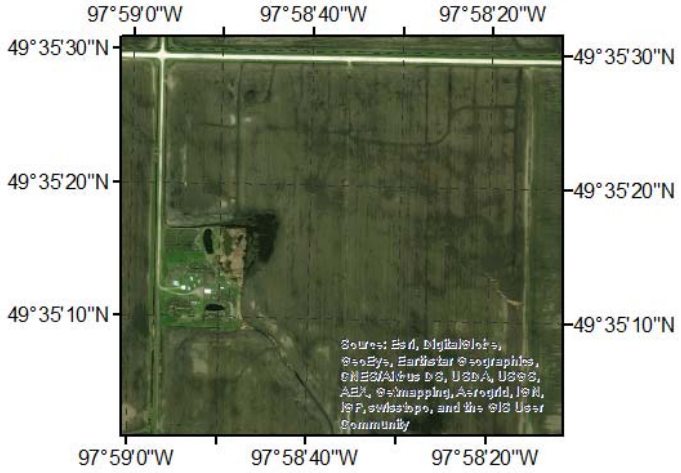

Field 71

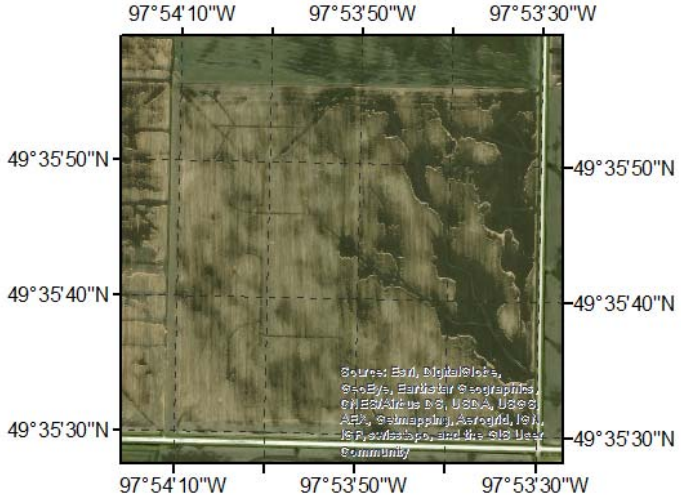

(a)

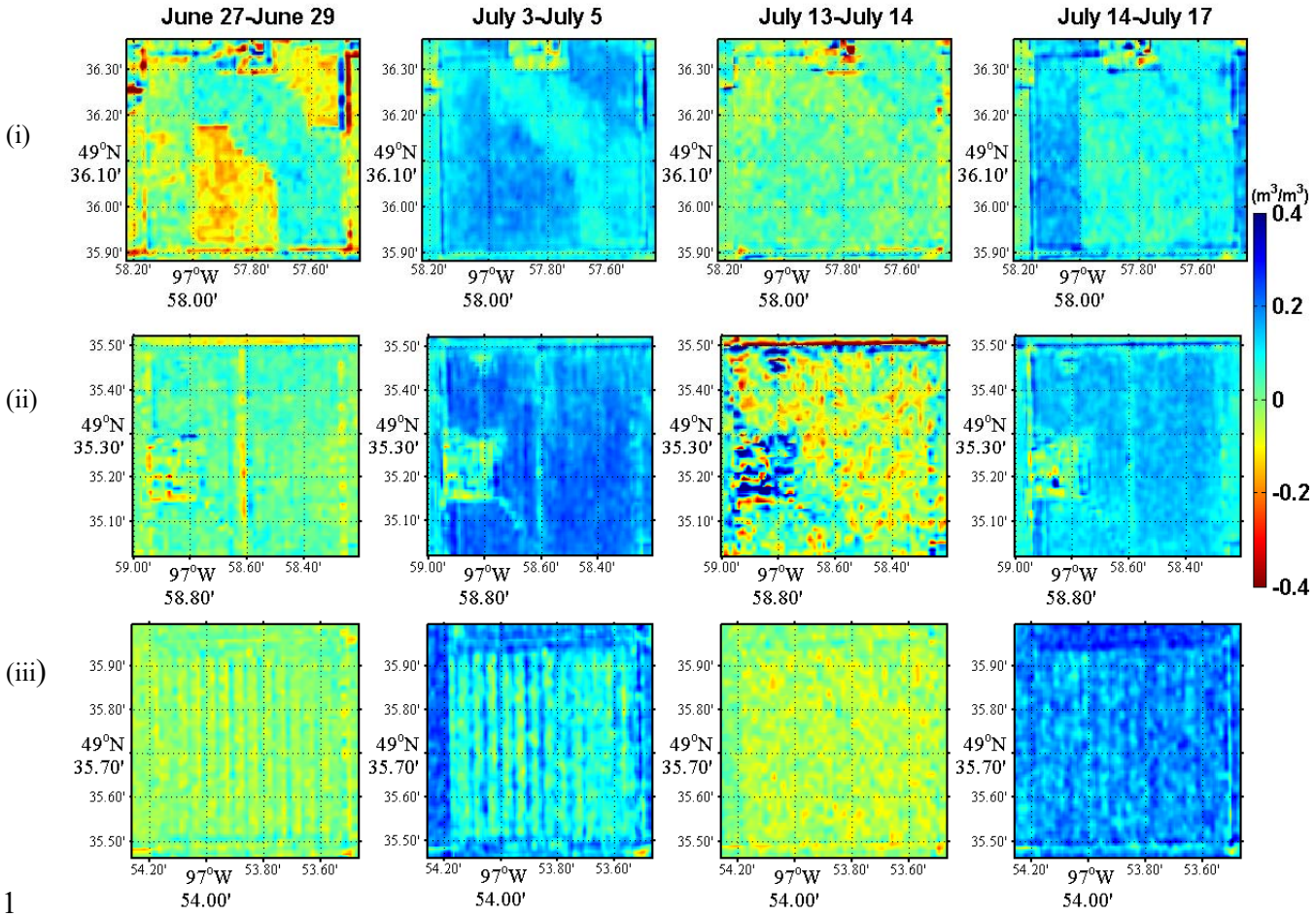

(b)

Figure 9. (a) Aerial photos (b) maps of disaggregated UAVSAR change in soil moisture (m^3/m^3) at 5 m resolution from June 29 to July 14 at three types of crop fields: (i) canola (field 62), (ii): soybeans (field 112), (iii): corn (field 71).

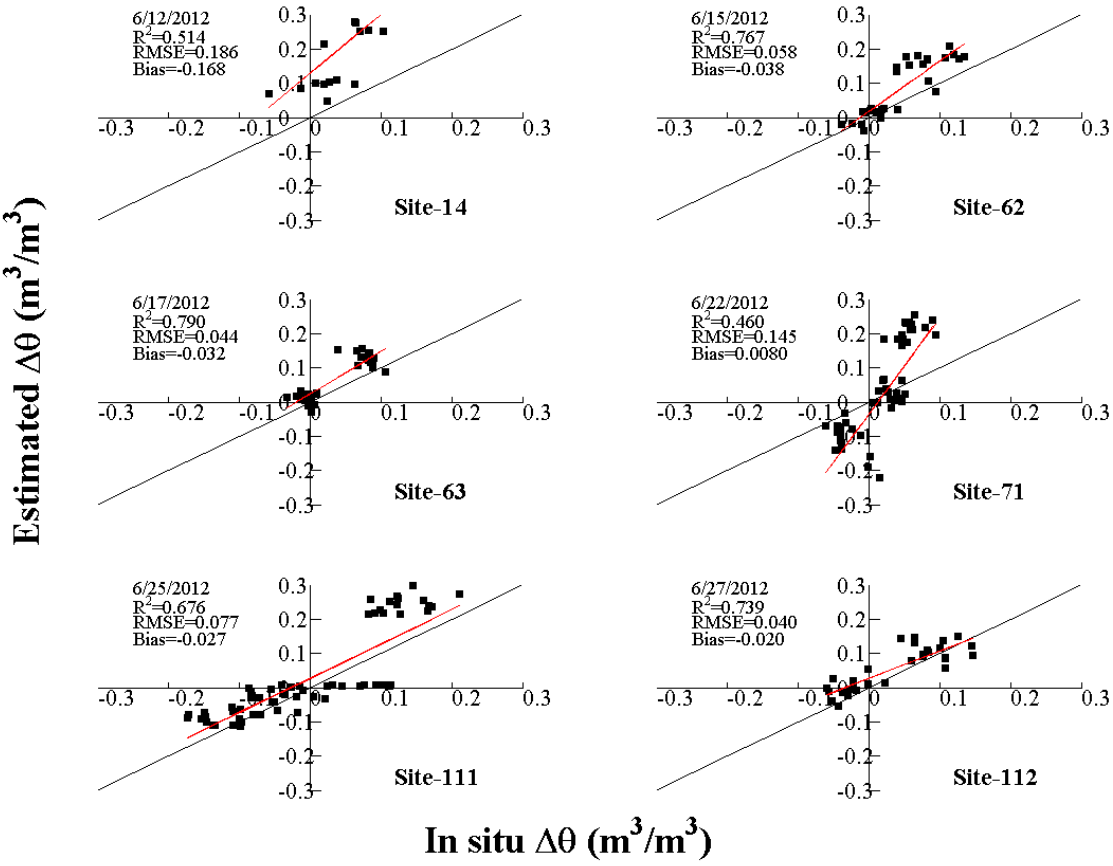

Figure 10. Validation of disaggregated UAVSAR change in soil moisture at 5 m resolution for July 3 - July 5, July 5 - July 8, July 8 – July 10, July 10 - July 13, at six sites representing different crop types.